Intermittency: A State that Precedes Thermoacoustic Instability

Chapter · January 2018

DOI: 10.1007/978-981-10-7449-3_14

2 authors:

Samadhan A. Pawar
Indian Institute of Technology Madras
24 PUBLICATIONS **56** CITATIONS
SEE PROFILE

Raman Sujith
Indian Institute of Technology Madras
235 PUBLICATIONS **2,301** CITATIONS
SEE PROFILE

Chapter 14
Intermittency: A State that Precedes Thermoacoustic Instability

Samadhan A. Pawar and R. I. Sujith

Abstract Thermoacoustic instability is a plaguing problem in confined combustion systems, where self-sustained periodic oscillations of ruinous amplitudes that cause serious damage and performance loss to propulsive and power generating systems occur. In this chapter, we review the recent developments in understanding the transition route to thermoacoustic instability in gaseous combustion systems and describe a detailed methodology to detect this route in a two-phase flow combustion system. Until now, in these combustion systems, the transition to such instabilities has been reported as Hopf bifurcation, wherein the system dynamics change from a state of fixed point to limit cycle oscillations. However, a recent observation in turbulent gaseous combustion system has shown the presence of intermittency that precedes the onset of thermoacoustic instability. Intermittency is a dynamical state of combustion dynamics consisting of a sequence of high amplitude bursts of periodic oscillations amidst regions of relatively low amplitude aperiodic oscillations. Here, we discuss the process of transition to thermoacoustic instability in the two-phase flow system due to change in the control parameter, a location of flame inside the duct. As the flame location is varied, the system dynamics is observed to change from a region of low amplitude aperiodic oscillations to high amplitude self-sustained limit cycle oscillations through intermittency. The maximum amplitude of such intermittent oscillations witnessed during the onset of intermittency is much higher than that of limit cycle oscillations. We further describe the use of various tools from dynamical systems theory in identifying the type of intermittency in combustion systems.

Keywords Spray combustion · Thermoacoustic instability · Type-II intermittency

S. A. Pawar · R. I. Sujith (✉)
Department of Aerospace Engineering, IIT Madras, Chennai 600036, India
e-mail: samadhanpawar@ymail.com

R. I. Sujith
e-mail: sujith@iitm.ac.in

S. Basu et al. (eds.), *Droplets and Sprays*, Energy, Environment, and Sustainability,
https://doi.org/10.1007/978-981-10-7449-3_14

14.1 Introduction

Thermoacoustic instabilities have been a topic of immense research for combustion community for several decades. Initially, such instabilities were observed in liquid and solid rocket motors in the mid of the twentieth century, and henceforth were reported in other propulsion engines (such as ramjet and afterburner), land-based gas turbine engines, boilers, industrial furnaces, etc. (Young 1995; Lieuwen and Yang 2005). These are self-sustained, high amplitude periodic oscillations in acoustic pressure generated mainly due to complex interaction between unsteady heat release rate from the flame and natural acoustic modes of the combustor (Lieuwen 2012).

The fluctuations in acoustic pressure lead to fluctuations in heat release rate either by modulating of the flame surface area, changing the fuel–air mixing ratio, varying the chemical kinetics or by affecting the underlying hydrodynamic flow-field of the combustor (Ducruix et al. 2003) (see Fig. 14.1). This oscillatory heat release, in turn, adds energy to acoustic field of the system, thus completing a feedback loop. According to Lord Rayleigh (1878), when the fluctuations in the heat release rate happen in phase with the acoustic pressure oscillations, a positive feedback is developed between the coupled processes of the combustor. Furthermore, when the net driving of the acoustic oscillations overcomes the overall damping in the system, the fluctuations in the system dynamics get amplified exponentially and saturate to high amplitude limit cycle oscillations when the driving matches with the nonlinear damping (Lieuwen and Yang 2005).

The intense growth in pressure amplitude may have serious damage to mechanical components of the combustor such as liners, fuel injectors, turbine blades, due to increased vibrations, or may degrade its performance (Culick and Kuentzmann 2006). Various control strategies have been developed over the years to either reduce the strength of such instabilities (McManus et al. 1993; Candel 2002; Culick and Kuentzmann 2006) or to forewarn their occurrences (Lieuwen 2005; Gotoda et al. 2014; Nair et al. 2013; Nair and Sujith 2014).

Although much progress has been made in understanding the physical mechanisms that cause thermoacoustic instability, their reliable prediction is still elusive.

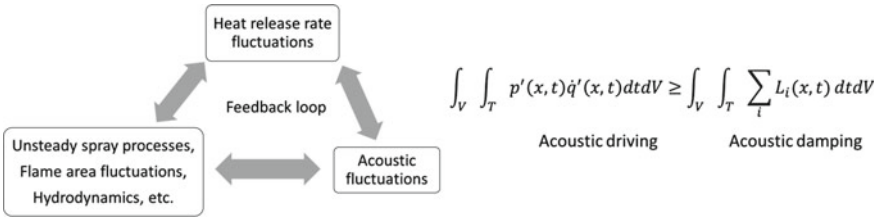

Fig. 14.1 Elementary processes leading to self-sustained thermoacoustic instability. The equation on the right side represents the criterion for the onset of thermoacoustic instability. When driving in the system is greater than damping, acoustic oscillations in the system grow to a state of limit cycle oscillations

In this context, the study on the transition of a thermoacoustic system from stable to unstable operation has received a growing interest in recent times. Here, stable operation corresponds to the state of combustion noise, and unstable operation represents the state of thermoacoustic instability (Smith and Zukoski 1985; Sterling and Zukoski 1987; Lieuwen 2002). The dynamics of a turbulent combustor observed during combustion noise comprises of low amplitude aperiodic oscillations, whereas that during thermoacoustic instability observed mostly in the form of high amplitude periodic (limit cycle) oscillations. In the case of laminar combustion systems, combustion noise corresponds to a steady state, while thermoacoustic instability may exhibit various forms such as quasiperiodic, period-2, period-k or chaotic oscillations in addition to limit cycle (Kabiraj et al. 2012; Kashinath et al. 2014).

The transition of combustor operation from combustion noise to thermoacoustic instability has been reported to occur via a Hopf bifurcation (Ananthkrishnan et al. 2005; Subramanian 2011; Sujith et al. 2016), wherein at a particular value of the control parameter, a sudden generation of periodic oscillations happens in the system dynamics from its steady-state value (Lieuwen 2002). However, a recent study on a turbulent combustor by Nair et al. (2014) showed that such transition of the combustor operation to thermoacoustic instability is not sudden, but happens gradually through the intermittent occurrence of bursts of periodic oscillations. They referred to such a transitional state as intermittency, wherein the system dynamics transitions alternately between low amplitude aperiodic oscillations and high amplitude periodic oscillations (see Fig. 14.2). It is to be noted that the amplitude of bursts observed during intermittency in their system was much lower than that of the limit cycle oscillations. Henceforth, various studies on gaseous combustion systems report the observation of intermittency in their respective systems (Gotoda et al. 2014; Unni and Sujith 2015; Kabiraj et al. 2016; Domen et al. 2015; Muugesan and Sujith 2015).

In thermoacoustics, the term intermittency was first introduced by Kabiraj and Sujith (2012). They reported the presence of high amplitude bursts of chaotic oscillations amidst regions of low amplitude periodic oscillations prior to a flame blowout. Furthermore, Unni and Sujith (2017) observed the presence of intermittency in

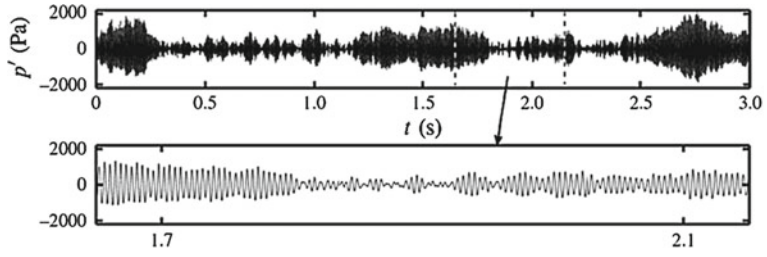

Fig. 14.2 The time series of acoustic pressure oscillations obtained during a state of intermittency from a bluff-body-stabilized turbulent combustor when $Re = 2.58 \times 10^4$ and equivalence ratio = 0.85. During intermittency, the bursts of high amplitude periodic oscillations occur in between the low amplitude aperiodic oscillations apparently in random manner. This is an example of intermittency observed prior to the onset of thermoacoustic instability (Nair et al. 2014)

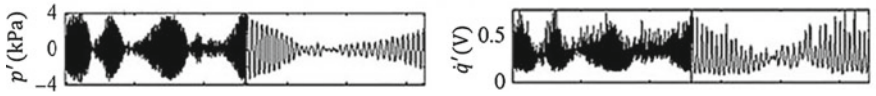

Fig. 14.3 The variation of acoustic pressure and heat release rate fluctuations obtained during a state of intermittency observed prior to a flame blowout in a bluff-body-stabilized turbulent combustor. The flow conditions were $Re = 2.28 \times 10^4$ and equivalence ratio = 0.47. During intermittency, both acoustic pressure and heat release rate fluctuations show apparently random switching between bursts of high amplitude periodic oscillations amongst the regions of low amplitude aperiodic oscillations (Unni and Sujith 2015)

turbulent combustor prior to the flame blowout, in which the bursts comprised of high amplitude periodic oscillations in between the regions of low amplitude aperiodic oscillations (refer Fig. 14.3).

The presence of intermittency is common in a variety of physical systems such as turbulent flows, Rayleigh–Bénard convection, plasma, lasers, and electronic circuits. Intermittency in dynamical systems theory is described as an irregular alternation of the behaviour of the system from periodic to chaotic oscillations (Hilborn 2000). Traditionally, there are three basic types of intermittency (i.e. type-I, type-II and type-III) which can cause the transition of system behaviour from periodic to chaotic state (Pomeau and Manneville 1980). In addition to these, various other types of intermittencies such as on-off, type-V, type-X, eyelet, and crisis-induced exist in the literature of dynamical systems (Elaskar and Del Río 2017). The type of intermittency is based on the specific kind of bifurcation a system has to undergo while transitioning from one dynamics to another. In this chapter, we will restrict ourselves only to three types: type-I, type-II and type-III intermittencies. Herein, type-I intermittency is associated with the saddle-node bifurcation, type-II intermittency with the subcritical-Hopf bifurcation and type-III intermittency with the period-doubling bifurcation.

Characterization of the type of intermittency is based on a few statistical methods such as (i) probability distribution of the duration between two consecutive bursts, and statistical variation of mean of this duration with control parameter, (ii) first return map and (iii) recurrence plot analysis (Pomeau and Manneville 1980; Schuster and Just 2006; Klimaszewska and Żebrowski 2009). Establishing the type of intermittency from experiments is necessary for improving the understanding of the phenomena and also in validating the models that predict the onset of thermoacoustic instability. In thermoacoustics, Kabiraj and Sujith (2012) observed type-II intermittency in the gaseous laminar premixed combustor (see Fig. 14.4), whereas Nair and Sujith (2013) mentioned the existence of type-II or type-III intermittency in the gaseous flame turbulent combustor. Furthermore, Unni and Sujith (2017) compared the intermittent oscillations observed in the turbulent combustor prior to thermoacoustic instability and flame blowout and confirmed the presence of type-II intermittency in both the cases. In addition, the presence of intermittency prior to thermoacoustic instability as well as flame blowout can aid in devising different

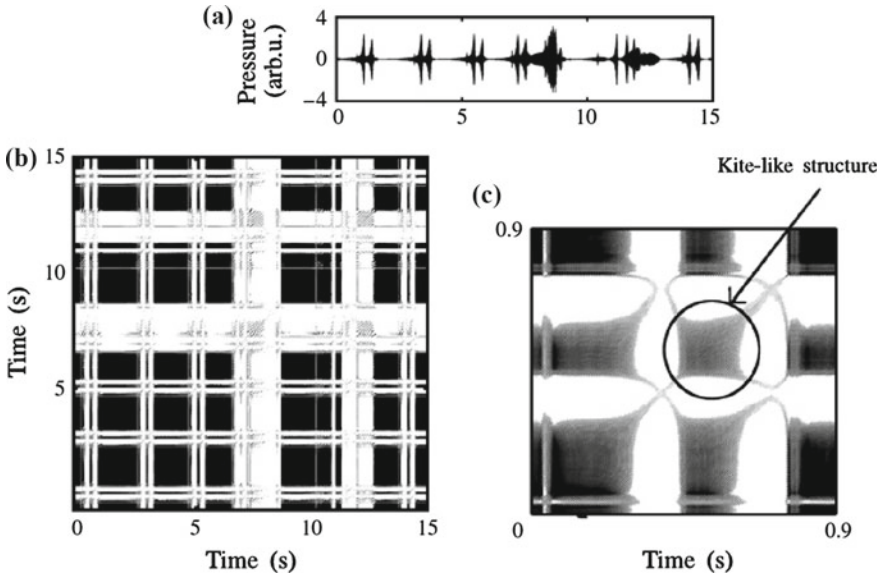

Fig. 14.4 **a** Time series of intermittency observed prior to flame blowout in a laminar combustor. Intermittency consists of bursts of chaotic oscillations amongst regions of low amplitude apparently periodic oscillations. **b** The recurrence plot of the intermittency signal depicting the black patches (corresponding to non-bursts regions) amongst the white patches (corresponding to burst regions). **c** An enlarged view of recurrence plot shows a kite-like structure with a long elongation at right upper corner depicting the property of type-II intermittency (Kabiraj and Sujith 2012)

control strategies that will forewarn the onset of such phenomena (Nair et al. 2013; Nair and Sujith 2014; Nair et al. 2014; Unni and Sujith 2015).

In spite of these recent advances in gaseous combustion systems in understanding the route to thermoacoustic instability, presence of such studies in spray combustion systems is negligible. Most combustion systems in practice utilize liquid fuels as a source of energy. Therefore, it is important to understand the phenomena of onset of thermoacoustic instabilities in such systems.

Spray combustors are susceptible to thermoacoustic instability because of the inherent unsteady processes involved in the combustion of such two-phase mixtures. Understanding the combustion of spray systems is complex as it has characteristics of premixed and diffusion flames at any time in different spatial regions of the combustor. The possible sources contributing to unsteadiness in the spray combustion are the methods of fuel injection, atomization and evaporation of droplets, mixing of fuel vapours with air and finally the burning of this mixture in the hot environment of the combustor (Young 1995; Culick 1988). Thermoacoustic instabilities in spray combustors are generally classified as injection-coupled instabilities, where the pressure oscillations in the combustor affect the injection pressure difference across the spray nozzle, thereby modulating the fuel flow rate entering into the combustor. The modulation in fuel flow rate fluctuates the equivalence ratio of combustion,

which in turn modulates the heat release rate in the system (Young 1995). Factors affecting the onset of thermoacoustic instability can be understood by simplifying the studies of spray–acoustic interaction. For instance, most of the studies in spray–acoustic interaction have been performed on single droplets. The presence of acoustic oscillations is simulated by imposing the external perturbations on the liquid droplets. The presence of acoustic field modifies the spray characteristics such as droplet diameter, velocity, evaporation and burning rates. Further, the response of droplets to the acoustic field depends highly on their spatial location inside the spray (Chishty 2005).

The experimental studies (Kumagai and Isoda 1955; Tanabe et al. 2000; Saito et al. 1996; Okai et al. 2000; Dattarajan et al. 2006) on the effect of acoustic oscillations on a single pendant drop showed that the increase in amplitude of acoustic forcing increases the rate of evaporation and burning of the droplet. Furthermore, for a moving droplet, the application of axial acoustic perturbations reduces its terminal velocity (Sujith et al. 1997). The modelling study by Duvvur et al. (1996) and Lei and Turan (2009) revealed that the vapourization of droplet acts as a main driving force in the generation of thermoacoustic instabilities, whereas the study by Anderson et al. (1998) indicated that the mean size of the droplets, special distribution of droplets of variable sizes in the combustor and periodicity in atomization of the spray also have an important effect on the onset of thermoacoustic instability. Besides, the position of spray in the combustor affects the intensity of acoustic oscillations generated in the system (Carvalho et al. 1989; Dubey et al. 1998). The presence of high amplitude acoustic oscillations reduces the length of the spray either by decreasing the droplets size (through increased evaporation rate) or by increasing the mean drag on the droplets Sujith 2005.

In summary, the main aim of these previous studies (numerical as well as experimental) was focused on characterizing the effect of acoustic oscillations (self-excited or externally forced) on the physical processes of the spray combustion observed during the state of thermoacoustic instability. On the contrary, the characterization of the route through which such instabilities are developed in spray combustor systems has not yet received much attention.

Recently, Pawar et al. (2016) performed a detailed study on the characterization of intermittency route to thermoacoustic instability in a laboratory-scale spray combustion system. The system comprised of a unified design of needle spray injector that generates a uniform droplet spray having velocity field only in the axial direction. Various tools from dynamical systems theory were used to understand dynamics of the combustor acquired at various locations of the flame inside the duct. In this chapter, we discuss the key results from their study on characterization of intermittency route to thermoacoustic instability and identification of type of intermittency in the spray combustion dynamics. Finally, the main takeaways from this study are summarized at the end of the chapter.

14.2 Tools from Nonlinear Dynamics

Dynamical systems are systems which evolve with time. The dynamics of such systems at every instant of time can be correctly determined from the knowledge of a fixed number of the dynamical variables, also known as state variables (Hilborn 2000). The time evolution of such variables can be expressed in the form $\mathrm{X} = \dot{\phi}(X)$, where the dot represents the time derivative. For a given set of initial conditions and the functional form (ϕ), the future dynamical states of the variable can be correctly determined from the above equation.

14.2.1 Phase Space Reconstruction

In order to describe the state of a practical dynamical system completely, infinite number of state variables are required. In contrast, the number of state variables available from such systems are limited and in the limiting case it is one. According to Takens′ delay embedding theorem (Takens 1981), it is possible to obtain all variables that are required to describe the state of a system using a time series of single observable. The dynamics of such systems can then be embedded into a higher-dimensional phase space using an appropriate value of embedding parameters such as the optimum time delay (τ) and the minimum embedding dimension (d) (Abarbanel et al. 1993). Suppose we have a single variable time series as $x(t) = x_1,\ x_2,\ x_3, \ldots\ldots\ldots,\ x_N$. Then the delay vectors are constructed as $Y_i(d) = [x(i), x(i+\tau), x(i+2\tau), \ldots\ldots\ldots, x(i+(d-1)\tau)]$, where $i = 1, 2, 3, \ldots\ldots, N-(d-1)\tau$. The plot of these delayed vectors represents the time evolution of every state of a given dynamical system in the d-dimensional phase space. The construction of phase space is highly dependent on the choice of τ and d.

14.2.1.1 Selection of Optimum Time Delay (τ) and Minimum Embedding Dimension (d)

The conventional way to select the optimum value of time delay (τ) is to choose the first local minimum of the average mutual information (AMI) (Fraser and Swinney 1986). The choice of time delay should be such that the resulting vectors obtained from lagging the samples of a given signal are independent of each other (Kantz and Schreiber 2004). If the time delay is very small, it will produce highly correlated vectors; on the contrary, if the time delay is very large, the resulting vectors would be completely uncorrelated with each other (Abarbanel et al. 1993). Now, consider a time series data of sampled variable $x(t)$ as $x(t_1),\ x(t_2), \ldots\ldots\ldots,\ x(t_i)$, and the corresponding delayed signal is $x(t_1+\tau),\ x(t_2+\tau),\ \ldots\ldots\ldots,\ x(t_i+\tau)$. The AMI of such signal is then calculated as

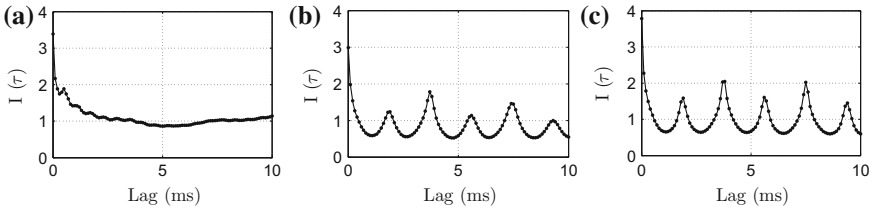

Fig. 14.5 The plots of average mutual information (AMI) corresponding to three signals acquired during the states of **a** combustion noise (x_f = 520 mm), **b** intermittency (x_f = 590 mm) and **c** thermoacoustic instability (x_f = 680 mm). The first local minima of the plot showing variation of AMI versus lag (shown by arrow) is chosen as the optimum value of time delay required for the reconstruction of phase space

$$I(\tau) = \sum_{x(t_i),\ x(t_i+\tau)} P(x(t_i), x(t_i+\tau)) \log_2 \left[\frac{P(x(t_i), x(t_i+\tau))}{P(x(t_i))P(x(t_i+\tau))} \right]$$

where $P(x(t_i))$ and $P(x(t_i+\tau))$ are the marginal probabilities, and $P(x(t_i), x(t_i+\tau))$ is the joint probability of occurrence of $x(t_i)$ and $x(t_i+\tau)$. Figure 14.5 represents the plots of average mutual information corresponding to three states of the combustion dynamics as combustion noise, intermittency and limit cycle oscillations.

The embedding dimension d is usually found from a method of false nearest neighbours (FNN) (Kennel et al. 1992). In this method, the percentage of closeness (measured in terms of distances) of the neighbouring points of the phase space trajectory is calculated in a given dimensional phase space, and then the value of this closeness is compared for the next dimensional space. If the value of the percentage is unchanged with an increase in the dimension, we assume that the attractor of the given signal is unfolded and the minimum embedding dimension required for the reconstruction of the phase space is achieved. The unfolding of all trajectories of the attractor is necessary to remove the possibility of false neighbours in the reconstructed phase space. If the neighbours are false, the changing of dimension from d to d+1 results in change in the number of neighbours of a given state point on the phase space trajectory. We, however, use another method suggested by Cao (1997), an optimization of FNN method, to find the embedding dimension.

If $Y_i(d)$ is the i^{th} reconstructed vector of d-dimensional space obtained using Takens′ delay embedding theorem (Takens 1981), we can define a new quantity $a(i,d)$ such that

$$a(i,d) = \frac{||Y_i(d+1) - Y_{n(i,d)}(d+1)||}{||Y_i(d) - Y_{n(i,d)}(d)||}$$

where $i = 1, 2, 3, ..., (N - d * \tau)$, and $||.||$ is the Euclidian norm. Further, $Y_i(d+1)$ is the i^{th} reconstructed vector in the $(d+1)$-dimensional space, and $n(i,d)$ is the nearest neighbour of $Y_i(d)$ in the d-dimensional space. Then, the mean of all $a(i,d)$ can be calculated as

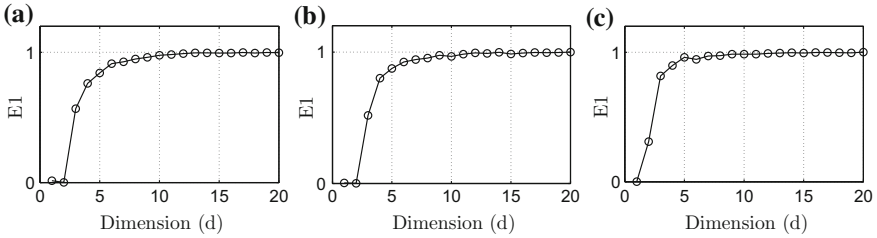

Fig. 14.6 The minimum embedding dimension is selected from the Caos method for three signals corresponding to the states of **a** combustion noise ($x_f = 520$ mm), **b** intermittency ($x_f = 590$ mm) and **c** thermoacoustic instability ($x_f = 680$ mm). The minimum value of embedding dimension d is chosen as the next dimension at which E1 saturates for the first time in the plot

$$E(d) = \frac{1}{(N-d)} \sum_{i=1}^{N-d\tau} a(i,d)$$

The variation of $E(d)$ due to change in the dimension from d to $d+1$ is expressed in terms of another quantity $E1(d)$ as

$$E1(d) = E(d+1)/E(d)$$

When $E1(d)$ is observed to stop changing after a dimension d_0, then the dimension $d_0 + 1$ can be chosen as the minimum embedding dimension required for the reconstruction of the phase space. Figure 14.6 shows the variation of $E1$ with the embedding dimension for the different states of combustion dynamics as combustion noise, intermittency and limit cycle oscillations.

14.2.2 Recurrence Plots and Quantification Analysis

Recurrence is a fundamental property of a deterministic dynamical system (Eckmann et al. 1987). The time evolution of the system dynamics can be captured by plotting the recurrence plot (RP) of a given time series. RP not only aids in visualizing the dynamics of a given system in a lower-dimensional space but also helps in detecting the hidden dynamical patterns present in the signal (Eckmann et al. 1987; Marwan et al. 2007). The concept of construction of RP is based on the process of recurrence of a phase space trajectory in the embedded space (see Fig. 14.7). Thus, in order to obtain RP for any given signal, we first need to reconstruct the phase space using the Takens′ delay embedding theorem (Takens 1981), and then from the choice of an appropriate value for the distance threshold, recurrence of the trajectory is quantified. The choice of size of the threshold is further dependent on the problem in hand. This threshold could be some fraction of size of the attractor (maximum or mean distance of the attractor) or could be a fixed number of nearest neighbours. Larger the size of

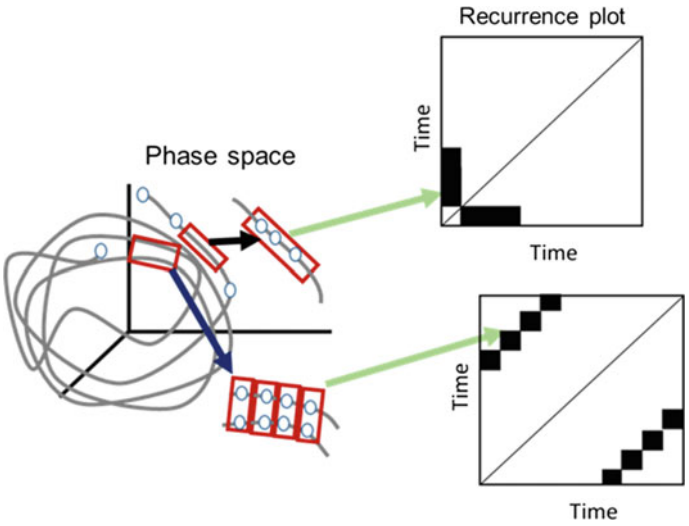

Fig. 14.7 The schematic of the construction of RP plot from the reconstructed phase space. The diagonal lines in the RP depict that two trajectories are running parallel to each other, whereas the vertical lines in RP demonstrate that more than one points of the same trajectory are recurring at the same time

threshold, more will be the recurrence of points in the phase space, hence we always need to choose an appropriate value of the threshold. The recurrence of the phase space trajectory can be quantified from following equation

$$R_{i,j} = \Theta(\varepsilon_i - ||x_i - x_j||); \quad i,j = 1,2,...,N_1$$

where $x_{i,j}$ are the delayed vectors, Θ is the Heaviside step function, $N_1 = N-(d-1)\tau$ is the total number of delayed vector, ε_i is a predefined threshold. Whenever the neighbouring trajectory of a given state point in the phase space falls within the threshold, it is marked as 1; otherwise, it is marked as 0 in the recurrence matrix. Thus, the recurrence plot is a graphical representation of black and white points, where black points correspond to $R_{i,j} = 0$ and white points correspond to $R_{i,j} = 1$.

Since RP is a visual inspection tool and its results are mostly qualitative in nature, Zbilut and Webber (1992) and Webber and Zbilut (1994) developed a recurrence quantification analysis (RQA) to establish robust conclusions from this method. RQA technique is mainly based on the quantification of the structural patterns such as diagonal lines, and vertical or horizontal lines present in the RP (Marwan et al. 2007). This quantification of structural patterns helps either in identifying the bifurcation points occurring in the complex dynamical systems or in deciding the deterministic nature of the system dynamics (Marwan et al. 2007). Based on this quantification, various statistical measures are developed, namely recurrence rate (*REC*), determinism (*DET*), laminarity (*LAM*), entropy (*ENTR*), longest diagonal line (L_{max}), longest

vertical line (V_{max}) and trapping time (TT). Out of these measures, we will be discussing the use two quantifiers, namely percentage of determinism ($\%DET$) and maximum value of diagonal line (L_{max}) in this chapter. We found that these measures are better than others in identifying the random or deterministic characteristics of the system dynamics (Marwan et al. 2007). Their values exhibit peak for periodic dynamics and have lower values for aperiodic dynamics. Further, these measures have been successfully used in the past for the detection of chaos-periodic transition in the same time series (Marwan et al. 2007).

Determinism (DET): It represents the quantification of lines that are parallel to main diagonal line in RP. It is the ratio of number of black points in RP that form a diagonal line to the total number of black points present in RP.

$$DET = \frac{\sum_{i=l_{min}}^{N} lP(l)}{\sum_{i=1}^{N} lP(l)}$$

where $P(l)$ is the histogram of the lengths l that form diagonal lines in RP and $l_{min} = 2$ points. Determinism is a measure of predictability of the dynamical system and shows a higher value close to 1 for the regular behaviour and lower value close to zero for the irregular behaviour.

Longest diagonal line (L_{max}): It is the length of the longest diagonal line, other than the main diagonal line, present in RP. The inverse of L_{max} is called divergence. It is also referred as an estimator for the largest positive Lyapunov exponent of the dynamical system (Marwan et al. 2007). Since the largest positive Lyapunov exponent is a measure of divergence of the phase space trajectory, its value is more for chaotic oscillations and less for periodic oscillations. The features of RQA in the detection of the determinism of the system dynamics are discussed in the results section.

14.3 Experimental Set-up

An experimental rig developed for studying the route to thermoacoustic instability in two-phase flow combustor is shown in Fig. 14.8. The detailed explanation of the experimental set-up description is available in Pawar et al. (2016). The experimental set-up consists of mainly four parts, i.e. fuel supply head, air input unit, needle injector and combustor. The fuel supply head is fitted at the top of the combustion system, whose main purpose is to store the fuel prior to entering into the combustor and also aid in equally distributing it through all needles of the injector. It is then followed by the air input unit, which is designed to supply air uniformly from all sides of the combustor. The combustor is a 1000 mm long quartz glass tube with inner diameter of 50 mm and thickness of 2.5 mm. Ethanol is used as a combustion fuel and is supplied from a gravity flow tank placed above the set-up. The pressurized air (1 bar gauge pressure) is provided by an air compressor.

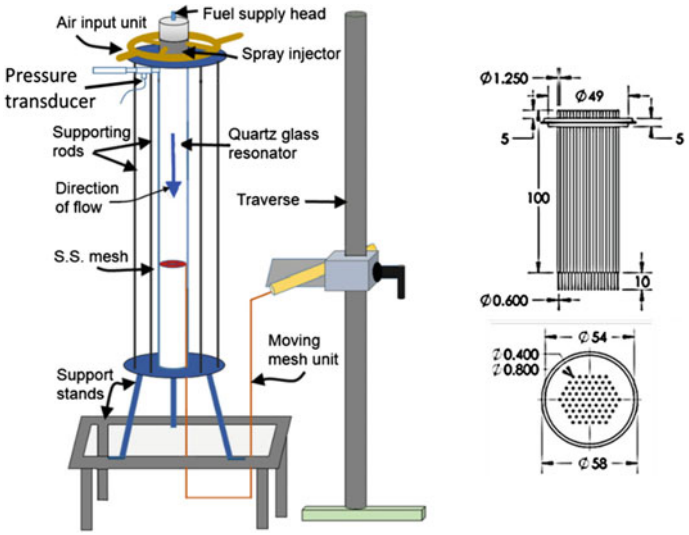

Fig. 14.8 Schematic of the experimental set-up of the spray combustion system is shown on the left side. The front and top views of the needle injector used in the generation of droplet spray are shown on the right side (Pawar et al. 2015). All dimensions are in mm

The injector consists of 70 stainless steel needles of 0.8 mm inner diameter, 1.25 mm outer diameter and 100 mm length. The size of the droplets is further reduced by fastening 10 mm long capillary tubes of size 0.4 mm inner diameter and 0.6 mm outer diameter at the end of primary needles of the injector. The needles are placed on the metal plate in such a way that each needle is fixed at the apex of the equilateral triangle of side 4 mm. This placing of needles helps in generating a uniform fuel flow across the combustor, and also in avoiding the interactions amongst droplets such as collision and coalescence, once they are injected.

Secondary atomization is achieved through two different size stainless steel wire meshes packed together as a single mesh unit. The mesh unit also serves as a function of anchoring the flame at a specific location inside the combustor. The relative position of the mesh unit from the bottom end of the combustor, defined as x_f, is varied as a control parameter.

Experiments were conducted at a constant equivalence ratio of 0.49 (uncertainty of 0.03). This is achieved by maintaining the fuel flow rate at 8 ccm and the air flow rate at 100 slpm. Fuel–air mixture is ignited from the bottom of the combustor using a pilot flame. Initially, during ignition, the mesh is lowered down to $x_f = 110$ mm and once the flame is anchored at the mesh, it is moved upward to $x_f = 480$ mm. At this position of the flame, the combustor is preheated at least for 7 min in every experiment before the start of data acquisition. Preheating minimizes the variation of temperature of the combustor wall from the time of ignition and ensures a constant wall temperature throughout the experiment.

Unsteady acoustic pressure fluctuations in the combustor are measured using a data acquisition system that consists of a pressure transducer, a signal conditioner and a data acquisition card. The pressure transducer (PCB piezotronics 103B02, the sensitivity of 223.4 mv/kPa, a resolution of 0.142 Pa) is fixed on a T-mount at a location of 140 mm from the injector plate, as shown in Fig. 14.8. The transducer is connected to the data acquisition card (NI PCI-6221) through a signal conditioner (PCB 480E09). A manual traverse arrangement is employed to move the mesh unit which, in turn, determines the location of the flame inside the combustor. The location of the flame holder (mesh unit) is varied in a step sizes of 10 mm throughout the experiment (least count on the traverse is 1 mm). Data is acquired for 30 s at the rate of 10 kHz at each location of the flame holder. A settling time of 30 s is ensured before the acquisition of data at every location of the flame. This settling time is necessary to avoid the transients associated with the change in the flame location.

14.4 Results and Discussion

14.4.1 Intermittency Route to Thermoacoustic Instability

In this section, we characterize the variation in the system dynamics due to change in the location of flame inside the combustor as a system parameter. The flame location is systematically varied from bottom to top half of the duct using a traverse mechanism. The dynamics of the combustor is analysed from the recordings of acoustic pressure acquired at each location of flame inside the system. Figure 14.9 displays a sequence of time series plots of the acoustic pressure fluctuations acquired at different locations of the flame inside the duct. With variation in the flame location, we notice that dynamics of the system transitions from a state of low amplitude aperiodic oscillations (stable operation) (Fig. 14.9a) to a state of high amplitude limit cycle oscillations (unstable operation) (Fig. 14.9p) via a regime of intermittency (Figs. 14.9b–o). Intermittency is the occurrence of a series of bursts of periodic oscillations in between the relatively silent regions of aperiodic oscillations (see Fig. 14.9q). During the onset of intermittency ($x_f = 540$ mm), we notice that the bursts are short-lived, large amplitude periodic oscillations. As the flame location is further increased, we note an increase in the size (duration) of the bursts which ultimately culminate in the limit cycle oscillations exhibiting sustained periodic oscillations in the pressure signal.

The amplitude spectrum of the acoustic pressure signals obtained during three major states of the combustion dynamics, i.e. combustion noise, intermittency and thermoacoustic instability is shown in Figs. 14.10a–c, respectively. We observe two low amplitude bands of broadband frequencies during the state of combustion noise. In these bands, the lower frequency band ($f_{dominant} = 97.9$ Hz) possibly corresponds to the heat release rate fluctuations present in the flame, whereas the larger frequency band ($f_{dominant} = 272.7$ Hz) shows the frequencies associated with the natural acoustic

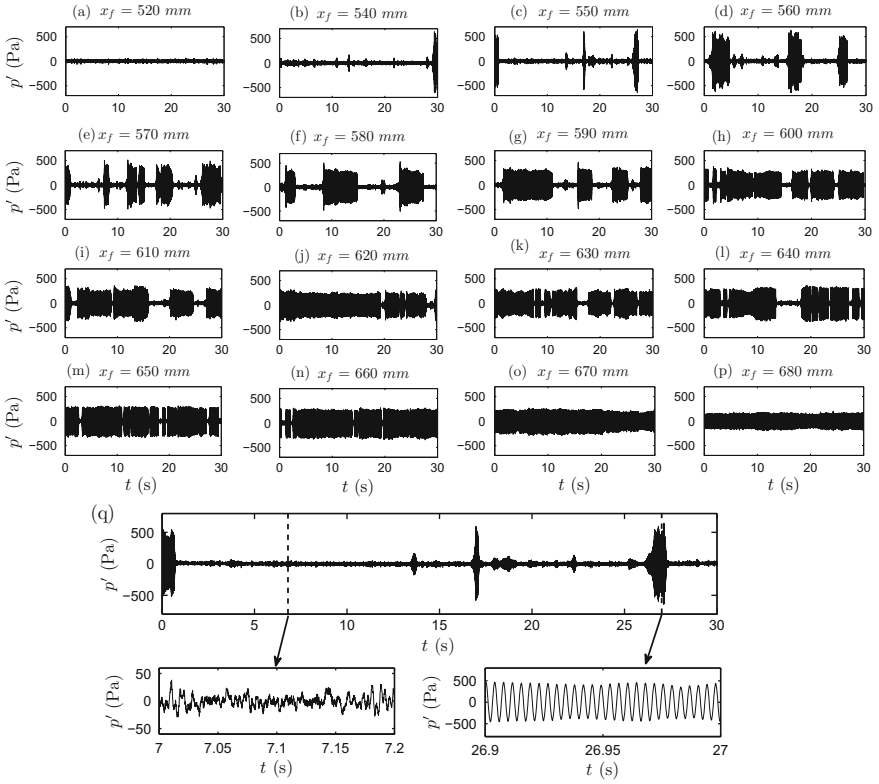

Fig. 14.9 Time series data of the acoustic pressure fluctuations acquired at different locations of flame in the combustor. **a** Combustion noise state ($x_f = 520$ mm), **b–o** intermittency state ($x_f = 540$ mm to $x_f = 670$ mm) and **p** limit cycle state ($x_f = 680$ mm). These plots show the intermittency route to limit cycle oscillations in a spray combustion system. **q** A magnified portion of intermittency signal obtained at $x_f = 550$ mm shows the low amplitude aperiodic oscillations and the burst of high amplitude periodic oscillations present in the signal (Pawar et al. 2015)

mode of the duct. As the system dynamics enter into a state of intermittency and limit cycle, a sharp frequency peak corresponding to the periodic oscillations is observed in the frequency range of 260 to 280 Hz. This frequency range matches nearly with the value of second longitudinal mode of the acoustic oscillations developed in a close–open configuration of the set-up (f_n = 3c/4L, where c = 360 m/s, L = 1 m). The transition of the system dynamics due to variation in the system parameter is further qualitatively analysed using a bifurcation diagram.

The bifurcation analysis of the acoustic pressure fluctuations is presented in Fig. 14.11. It shows the variation of the global maxima (p'_{max}) (Fig. 14.11a) and the root-mean-square (Fig. 14.11b) values of the acoustic pressure signal with change in the location of flame holder inside the combustor. The plot is divided into three regions: region I—combustion noise, region II—intermittency and region III—

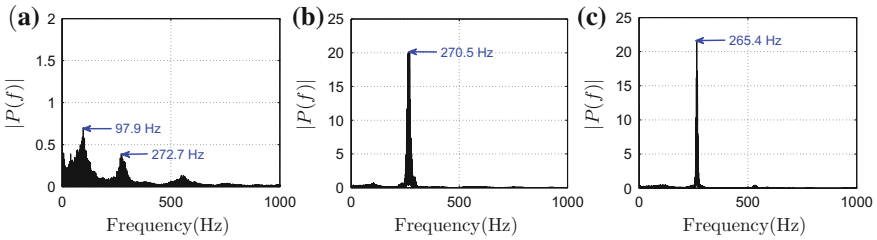

Fig. 14.10 The amplitude spectrum of the acoustic pressure signals acquired during the state of **a** combustion noise ($x_f = 520$ mm), **b** intermittency ($x_f = 590$ mm) and **c** limit cycle ($x_f = 680$ mm) oscillations in the combustor

thermoacoustic instability. During stable operation of the combustor, up to $x_f = 530$ mm, low amplitude aperiodic oscillations are observed (see region I of Figs. 14.11a, b). At $x_f = 540$ mm, as the system dynamics enters into a zone of intermittency, a jump in the maximum amplitude of the acoustic pressure signal is noticed. This sudden hike in the pressure amplitude is due to the occurrence of high amplitude bursts of periodic oscillations from the background of low amplitude aperiodic oscillations. This point is further referred to as the onset of intermittency in the system dynamics. The intermittent state of oscillations is observed from $x_f = 540$ mm to $x_f = 670$ mm, as shown in region II of Fig. 14.11a. Finally, for $x_f = 680$ mm and $x_f = 690$ mm (see region III of Figs. 14.11a, b), the system enters into a region of limit cycle oscillations, where sustained periodic oscillations are observed in the system dynamics. We found that during the onset of intermittency, the maximum amplitude of bursts (in the start of region II of Fig. 14.11a) is much higher in magnitude than that of the limit cycle oscillations (region III of Fig. 14.11a). We notice a decrease in maximum amplitude of acoustic pressure oscillations from the point of onset of intermittency to that of limit cycle oscillations as seen in Fig. 14.11a and also in the time series plots presented in Fig. 14.9. However, this behaviour of decrease in the pressure amplitude is not effectively seen in the plot of variation of p'_{rms} with flame location (see Fig. 14.11b). This is because p'_{rms} averages out the values of high amplitude pressure oscillations that occur for a short duration amongst the lengthy regions of low amplitude aperiodic oscillations during the onset of intermittency.

Nair et al. (2014) reported the observation of intermittency route to thermoacoustic instability in their turbulent gaseous flame combustor. They noticed that the root-mean-square values of the acoustic pressure fluctuations (p'_{rms}) increase continuously from the point of onset of intermittency to limit cycle oscillations due to change in Reynolds number of the flow in the system. In stark contrast with Nair et al. (2014), we witness that the amplitude (local maxima as well as root-mean-square values) of intermittent oscillations of acoustic pressure fluctuations is much higher than that observed for limit cycle oscillations. Historically, it was considered that limit cycle oscillations are dangerous to the combustion systems. The problems associated with high amplitude limit cycle oscillations have been described by various researchers in the past (McManus et al. 1993; Culick and Kuentzmann 2006).

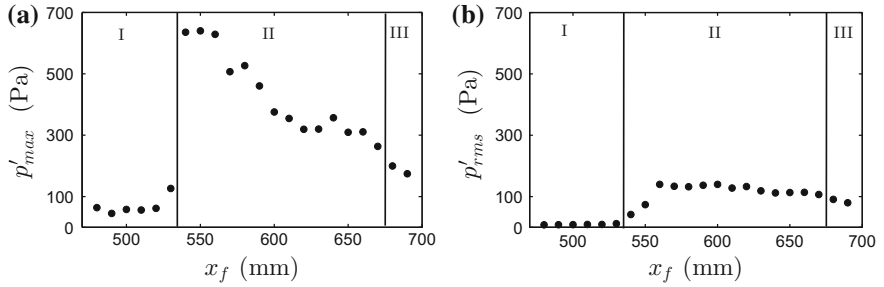

Fig. 14.11 The variation of **a** a global maximum (p'_{max}) and **b** a root-mean-square (p'_{rms}) value of the acoustic pressure signal versus the location of flame (x_f) inside the combustor. The plots are divided into three distinct regions of system dynamics as (I) low amplitude aperiodic oscillations, (II) intermittency and (III) limit cycle oscillations (Pawar et al. 2015)

The continuous loading of the system during the sustained instability state may lead to severe vibrations of mechanical parts of the combustor that either induce thermal and hoop stresses in the combustor walls, cause compressor surge or damage turbine blades. The accumulation of these stresses over a period of time may lead to catastrophic failure of the engine during its operation. However, the effects of high amplitude intermittent loads on the structural properties of the engine need to be investigated in future studies.

14.4.2 Qualitative and Quantitative Analysis of Intermittency Route

In this section, the dynamics of the acoustic pressure fluctuations acquired at different states of the combustor operation is explored through tools from dynamical systems theory. Thermoacoustic systems are nonlinear in nature, wherein the nonlinearity stems mainly from the coupled interaction between the acoustic field of the duct and the unsteady heat release present in the flame (Lieuwen 2002). Using the approach of nonlinear dynamics, we can visualize the single variable time series of the experimental signal into a higher-dimensional reconstructed phase space. Such phase space is reconstructed using delay embedding theorem proposed by Takens (1981). Figure 14.12 shows three-dimensional phase portraits of the acoustic pressure fluctuations (p') measured at three states of the combustor operation which are combustion noise, intermittency and thermoacoustic instability. In Fig. 14.12a, the phase portrait of p' acquired during the combustion noise state is shown. As the acoustic pressure oscillations are aperiodic in nature, the phase portrait corresponding to this state displays a clutter of trajectories. During intermittency, it is observed that the phase space trajectory continuously switches between high amplitude periodic (outer regular circle) and low amplitude aperiodic (centre disorder region)

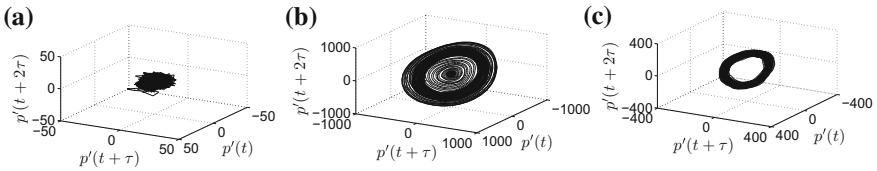

Fig. 14.12 Reconstructed phase portrait of a portion of the pressure time series (0.5 s) obtained during three different dynamical states system dynamics such as **a** combustion noise (x_f = 520 mm; $\tau = 3$, $d = 11$), **b** intermittency (x_f = 590 mm; $\tau = 10$, $d = 9$) and **c** thermoacoustic instability (x_f = 680 mm; $\tau = 10$, $d = 9$) (Pawar et al. 2015)

oscillations as shown in Fig. 14.12b. During limit cycle oscillations, the phase space of the signal displays a thick circular structure (see Fig. 14.12c), in which the thickness of the circle is caused by the amplitude variation of the acoustic pressure oscillations observed during limit cycle state.

We further characterize the nature (random or chaotic) of acoustic pressure fluctuations obtained during the combustion noise state. Such classification of the signal observed during this state is necessary to develop an appropriate model required for the analysis of the combustor dynamics. Various methods are available in the literature to distinguish chaotic signal from a noisy one. These include Lyapunov exponent, 0–1 test, determinism test (Kantz and Schreiber 2004). However, in the present analysis, we discuss the use of an approach based on RPs. The advantage of this method is that it requires a shorter time series, unlike other cases, to analyse the data. Further it helps in better visualization of divergence of the phase space trajectory compared to the other methods.

14.4.2.1 Detection of Chaos

In this section, the difference between the random process and the chaotic process is examined by using RPs and the measures based on its quantification. Towards this purpose, we have performed a comparison test of the experimental data obtained at x_f = 520 mm and the data generated by random shuffling of the experimental signal using a method of surrogate analysis (Theiler et al. 1992). This test aids in distinguishing the nonlinear behaviour of the real-world data from the linear process by using an appropriate null hypothesis. In order to reject the hypothesis, a significance of the test against the null hypothesis is examined. Many realizations of the null hypothesis are generated, and the significance of the test is estimated empirically. This check is important in showing that the underlying dynamics present during the aperiodic state of oscillations is a deterministic chaos and not a random noise.

The structural patterns present in RPs further represent the typical behaviour of the phase space trajectory. The long lines parallel to the main diagonal exemplify a periodic (deterministic) process, whereas homogeneously distributed black points indicate white noise (random) process. On the other hand, a chaotic process is shown

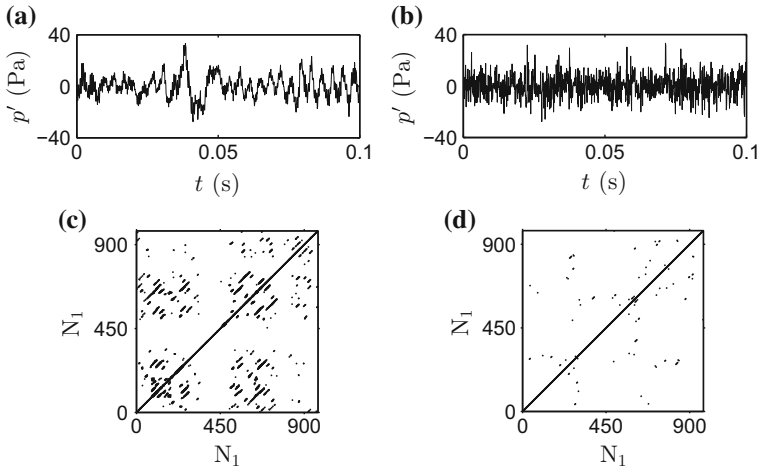

Fig. 14.13 **a** The recurrence plots of the pressure signal measured at $x_f = 520$ mm and **b** the signal obtained by random shuffling of the pressure data in a. **c** The short diagonal lines parallel to main diagonal confirm the underlying dynamics is chaotic, and **d** grainy structure with random distribution of single points in RP shows the dynamics is random. $N = 1000$, $\tau = 3$, $d = 10$, $\varepsilon = 30\%$ of the mean diameter of the attractor, and $N_1 = 973$

by the apparently random distribution of short diagonal lines along with a few isolated black points in RP (Marwan et al. 2007). The characteristic of chaotic oscillations is that the neighbouring trajectories in the phase space of such signals remain nearby for a short duration and then diverge exponentially at far distances. Hence, when the trajectories are adjacent, they recur inside the recurrence threshold and do not recur after the exponential divergence. Conversely, in the case of random signals, every event of the signal is independent of the previous one. Hence, for such signals, the possibility of recurrence of the phase trajectory is very low.

The RPs of the aperiodic oscillations observed during combustion noise state (Fig. 14.13a) and the signal generated by random shuffling of data points of this signal by surrogate analysis (Fig. 14.13b) are shown in Fig. 14.13. During the random shuffling of data points, the statistical properties of the signal such as sample mean, variance and autocorrelation function are maintained same as that of the original signal used for the construction. In Fig. 14.13c, we notice the presence of short (broken) diagonal lines along with few single points in RP suggesting the possibility of chaotic oscillations during the combustion noise state. In the contrast, Fig. 14.13d shows the grainy structure with the apparently random distribution of isolated black points in RP confirming the noisy behaviour of the oscillations in the signal.

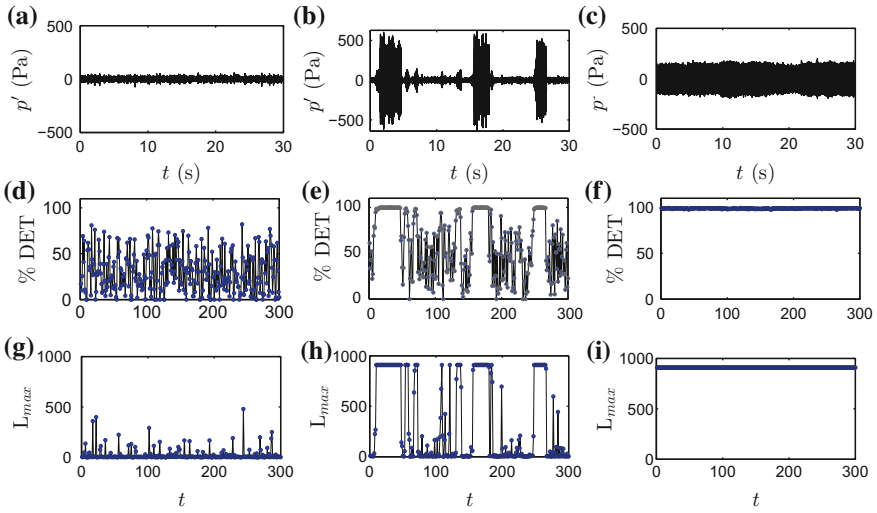

Fig. 14.14 **a–c** The pressure time signal obtained at x_f= 520 mm (chaotic), x_f = 560 mm (intermittency) and x_f = 680 mm (limit cycle) respectively. **d–i** The variations of $\%DET$ and L_{max} along the time axis for a time window of 1000 data points. The values of $\%DET$ and L_{max} show apparently random fluctuations for chaotic oscillations and a constant line at relatively maximum value for periodic oscillations. The values of $\%DET$ are always much higher than zero, confirming that the underlying dynamics during low amplitude state is deterministic. $N = 300000$, $\tau = 10$, $d = 10$, $\varepsilon = 25\%$ of the mean diameter of the attractor and a data window of 1000 points

14.4.2.2 Detection of Dynamical Transitions from Chaos to Period Using RQA

We further use measures of recurrence quantification analysis, mainly based on the characterization of diagonal patterns from RP (i.e. $\%DET$ and L_{max}), to investigate the transition points of the system dynamics from aperiodic to periodic oscillations and vice versa. In order to do this, we divide the entire time series into non-overlapping time windows of 1000 data points. The values of $\%DET$ and L_{max} are then calculated for each time window and plotted against the number of windows for the given signal. Figure 14.14 shows the variation of these measures obtained for combustion noise (Fig. 14.14a), intermittency (Fig. 14.14b) and thermoacoustic instability (Fig. 14.14c) states. The length of the diagonal line has a direct connection with determinism property of the system dynamics. The points along the diagonal line show evolution of the similar situations in the future time. Moreover, the short diagonal lines indicate the short-term predictability and long diagonal lines demonstrate the long-term predictability of the system dynamics.

The values of $\%DET$ are sufficiently higher than zero for every time window indicating the possibility of chaotic oscillations Marwan et al. 2007 in the underlying dynamics of aperiodic oscillations observed during the combustion noise state (see Figs. 14.14d, g). The values of $\%DET$ and L_{max} reach a maximum during

the periodic phase of oscillations. During the state of intermittency, the values of recurrence quantifiers display lower value for aperiodic oscillations and reach a maximum value during periodic oscillations (see Figs. 14.14e, h). For a proper value of the recurrence threshold, the temporal variation of these recurrence measures will clearly manifest the transition points of the system dynamics from aperiodic to periodic oscillations, and vice versa, in the time series displaying intermittency. This is observed from the strong change in $\%DET$ and L_{max} values across the transition point shown in Figs. 14.14e, h. The ability of these RQA measures in discerning even low amplitude periodic oscillations from the low amplitude aperiodic oscillations present during intermittency is also illustrated in Figs. 14.14e, h. However, such transitions from aperiodic to periodic oscillations or vice versa, for the bursts of low amplitude periodic oscillations, are difficult to identify from the visual inspection of the phase portraits of such signals. For the periodic oscillations (or thermoacoustic instability) of any amplitude (low or high) in the pressure signal, the values of $\%DET$ and L_{max} stay at maxima throughout the signal, as seen in Figs. 14.14f, i. Thus, the periodic oscillations observed during thermoacoustic instability establish the highest predictability by showing only continuous diagonal lines in the RP.

The transition of system dynamics from combustion noise to thermoacoustic instability can be quantitatively explained by plotting the time average values of $\%DET$ and L_{max} with control parameter as shown in Fig. 14.15. The values of $\%DET$ and L_{max} are calculated for every time window of 1000 data points and averaged over the entire signal. The average value of $\%DET$ is close to 1 for oscillations during thermoacoustic instability, as the observed dynamics during this state is completely periodic; on the contrary, it is around 0.2 for the combustion noise state, as the observed dynamics is aperiodic. During intermittency, the value of this measure lies in between these extreme values. Similar behaviour is observed in the variation of average value of L_{max}. The increase in the average values of $\%DET$ and L_{max} with control parameter indicates the increase in predictability of the system dynamics. Other types of RQA measures, namely recurrence rate, entropy and trapping time

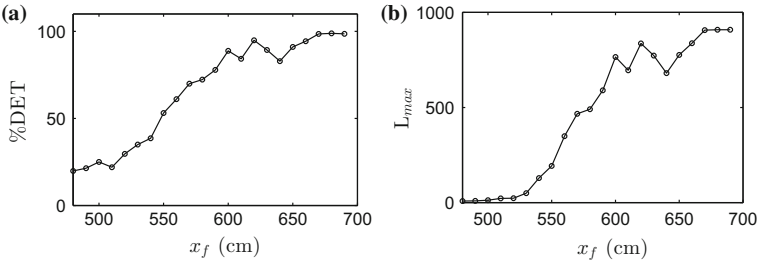

Fig. 14.15 **a**, **b** The variation of average values of the percentage of determinism ($\%DET$) and the maximum diagonal line (L_{max}) with location of control parameter shows a smooth transition of system behaviour from low amplitude chaotic oscillations to sustained limit cycle oscillations. The maximum value of $\%DET$ and L_{max} at $x_f = 680$ mm and $x_f = 690$ mm indicate that the system is having highest determinism value ($\tau = 10$, $d = 10$, $\varepsilon = 25\%$ of the mean diameter of the attractor)

have been previously used by Nair et al. (2014) to forewarn the impending instability of the practical gas turbine combustor. Controlling the operation of combustor at the onset of first burst in the pressure signal, by detecting the changes in $\%DET$ and L_{max} plots, will help in protecting the system components from any further damage.

14.4.3 Detection of Type of Intermittency

In the following analysis of intermittency, a low amplitude aperiodic regions present between the consecutive bursts are defined as the turbulent phases and the regions of high amplitude bursts of periodic oscillations are called as the laminar phases. The terms turbulent phase and laminar phase are completely different from the terminology of turbulent flow and laminar flow used in the fluid mechanics. The length of the turbulent phases (T) present in the unsteady pressure signal is determined to quantify the type of intermittency. Furthermore, the conventions of laminar and turbulent phase used in the present analysis may contradict with that used in the literature of dynamical systems theory, wherein the bursts of chaotic oscillations are described as turbulent phases and the regions of periodic oscillations observed in between the bursts are described as laminar phases.

Figure 14.16 shows a portion of the acoustic pressure signal acquired during a state of intermittent dynamics. For the calculation of length of turbulent phase (T), we adopt a method suggested by Hammer et al. (1994). Using this approach, an amplitude threshold is expressed in terms of fraction of maximum pressure such that threshold $= max(P)/(2^n)$, where P is the maximum value of the pressure amplitude of the signal and $1 \leq n \leq 6$. Here, we present the results corresponding to $n = 4$, which is equal to a pressure amplitude threshold of 54 Pa. The duration in the acoustic pressure signal having an amplitude below the selected threshold (i.e. the signal length between consecutive bursts) is defined as the length of the turbulent phase, as described in Fig. 14.16. The turbulent phase starts when the last waveform

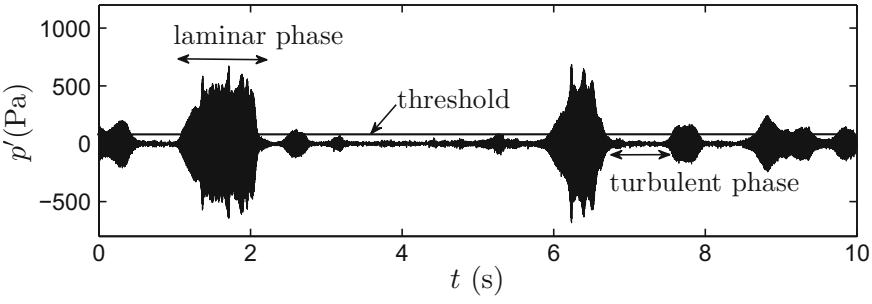

Fig. 14.16 The intermittency signal consists of low amplitude turbulent phases in between consecutive high amplitude laminar phases. A pressure threshold demarks the high amplitude periodic oscillations from low amplitude aperiodic oscillations (Pawar et al. 2015)

of the periodic burst falls below the threshold and ends when the first waveform of the next burst exceeds the threshold. These turbulent lengths are binned to calculate their probability distribution (using histogram) near the critical point. The critical point (x_{f0}) is the value of control parameter corresponding to the onset of intermittency. In our case, the onset of intermittency was observed at $x_{f0} = 540$ mm. In order to characterize the type of intermittency, a separate experiment was performed to acquire a sufficient number of bursts near the critical point. The acquisition of such lengthy data is necessary to confirm the statistical convergence of the obtained results. Towards this purpose, the data was acquired for 300 s at a sampling rate of 3 kHz.

14.4.3.1 Distribution of the Length of the Turbulent Phase

The histogram of the length of the turbulent phase present in the acoustic pressure signal acquired at $x_f = 540$ mm is shown in Fig. 14.17. An optimum pressure amplitude threshold of 54 Pa was chosen to ensure that no aperiodic oscillations are captured inside the threshold. Figure 14.17 shows an exponential decrease in the probability distribution of the length of the turbulent phase. Such distribution is consistent with the distribution shown for type-II and type-III intermittencies (Xiao et al. 2009; Frank and Schmidt 1997; Sacher et al. 1989; Schuster and Just 2006). Therefore, this distribution of turbulent lengths eliminates the possibility of type-I intermittency, which is characterized by a bimodal distribution (Schuster and Just 2006; Feng et al. 1996).

Figure 14.17b shows the variation of the average length of the turbulent phase with the normalized control parameter. Since the appearance of bursts is apparently random during intermittency, the average length of the turbulent phases $< T >$ is used as a representative of the total lengths of turbulent phases existing in the corresponding pressure signal. The normalized flame location is given by $r = (\tilde{x}_f - \tilde{x}_{f0})/\tilde{x}_{f0}$, where $\tilde{x}_f$ $(= x_f/L)$ and $\tilde{x}_{f0}$ $(= x_{f0}/L)$ are the locations of the

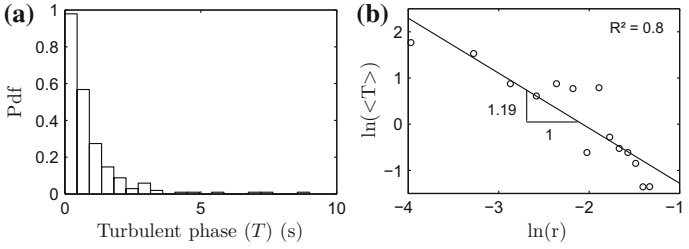

Fig. 14.17 **a** The distribution of the length of the turbulent phases obtained at $x_f = 540$ mm shows an exponential tail. **b** A log–log plot of the average value of the length of the turbulent phase $< T >$ versus the normalized flame location (r) shows a scaling law behaviour of type-II intermittency Pawar et al. (2015)

flame holder, measured from open end of the combustor (x_f) and that corresponding to the onset of intermittency (x_{f0}) respectively, normalized by the length of the duct (L). The mean duration of the turbulent phase plotted against each location of the flame holder on a log–log plot shows a power law behaviour. The variation of $< T >$ with r shows a linear relationship of slope -1.19, which is close to the theoretical value predicted for type-II and type-III intermittencies, i.e. $< T > \sim r^{-1}$ (Pomeau and Manneville 1980; Sacher et al. 1989; Chatterjee and Mallik 1996; Ringuet et al. 1993); on the contrary, for type-I intermittency, it is $< T > \sim r^{-1/2}$ (Pomeau and Manneville 1980; Feng et al. 1996). This statistical distribution again rules out the possibility of type-I intermittency in our experimental data. The difference in the values of slope obtained from theory (-1) and from experiments (-1.19) could be the result of finite length of the experimental signal, unavoidable noise in experiments and also in measurements, and challenge in detecting the length of turbulent phases accurately.

14.4.3.2 Analysis Using First Return Map

Finally, a method of first return map is used to differentiate type-II intermittency from type-III intermittency (Sacher et al. 1989). It is a two-dimensional plot between first local maxima of the signal versus next local maxima. Here, we plot the local maxima, say X_n, of the oscillations in laminar phases present in between the consecutive turbulent phases, is plotted against the next local maxima, i.e. X_{n+1}. In the first return map, the scatter of points along the main diagonal line is observed (Fig. 14.18a), whereas the evolution of these points shows a spiral-like structure in the plot (Figs. 14.18b, c). Such spiralling structure of the phase space trajectory is a typical characteristic property of type-II intermittency (Frank and Schmidt 1997; Sacher et al. 1989; Ringuet et al. 1993). In Fig. 14.18b, the evolution of some of the initial points from Fig. 14.18a is plotted to show the spiralling behaviour of the phase space trajectory. For type-I intermittency, the first return map shows an open channel between the diagonal line and the phase space trajectory (Schuster and Just 2006; Feng et al. 1996), whereas for type-III intermittency, it is represented by a two-fold trajectory crossing the diagonal line with increasing trend for sub-harmonic amplitude and decreasing trend for fundamental amplitude (Schuster and Just 2006; Griffith et al. 1997), which are different from that shown in Fig. 14.18. This confirms the presence of type-II intermittency in the present study.

14.4.3.3 Investigation Based on Recurrence Plot

Another way to identify the type of intermittency is based on RP analysis (Klimaszewska and Żebrowski 2009). The occurrence of different types of intermittency will result in various characteristic patterns in the RP. The recognition of the structure in RP will help in determining the type of intermittency. We have used a recurrence quantification analysis software package developed by Hasson et al. (2008)

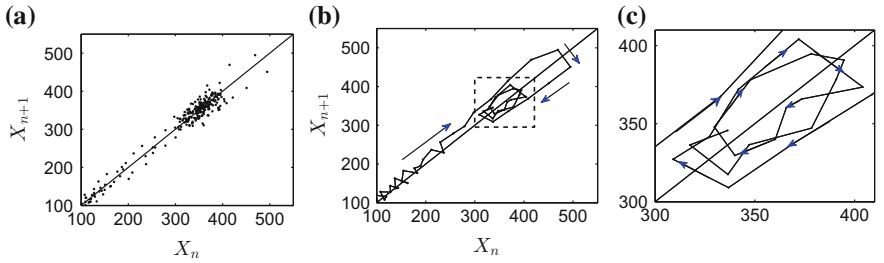

Fig. 14.18 **a** First return a map of the intermittency signal shows a scatter of points along the diagonal line. **b**, **c** The time evolution of these points indicates a spiralling behaviour of the trajectory, which confirms the possibility of type-II intermittency in the system dynamics (Pawar et al. 2015)

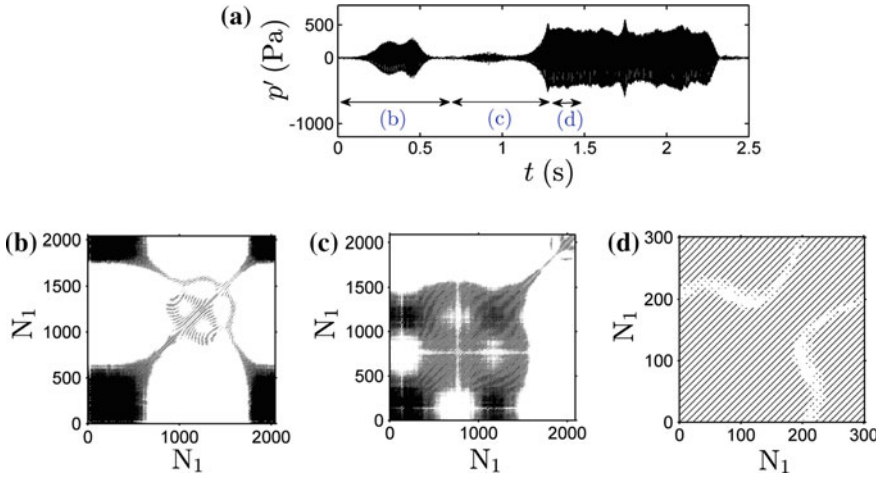

Fig. 14.19 **a** A portion of the signal displaying intermittency. **b**–**d** Recurrence plots (RP) obtained from different regions of the intermittency signal. **c** RP shows a kite-like structure of type-II intermittency. Data points $(N) = 7500$, $\tau = 3$, $d = 10$, $\varepsilon = 20\%$ of the mean diameter of the attractor (Pawar et al. 2015)

to obtain RPs of the experimental signal. Figures 14.19b–d show the RPs of small portions of the time series displaying intermittency (see Fig. 14.19a) obtained at x_f = 540 mm. Figure 14.19c shows a kite-like structure, representative of type-II intermittency, observed during the transition of system dynamics from low amplitude aperiodic to high amplitude periodic oscillations. A sinusoidal shape at the right upper corner of the kite with white perforations inside the kite (Fig. 14.19c) is the characteristic of type-II intermittency. Figure 14.19d shows the diagonal lines parallel to main diagonal line representing the periodic behaviour present in the burst. Kabiraj and Sujith (2012) and Unni and Sujith (2017) reported the presence of such

kite-like structures, observed prior to blowout of the flame, for confirming type-II intermittency in gaseous laminar premixed and turbulent partially premixed combustors, respectively.

14.5 Conclusion

In this chapter, we discuss the observation of intermittency route to thermoacoustic instability in a laboratory-scale spray combustion system due to variation in the flame location as the control parameter. The intermittency is characterized by the presence of high amplitude bursts of periodic oscillations amongst regions of low amplitude aperiodic fluctuations. The analysis of recurrence plot and recurrence quantification of the experimental data proves that the low amplitude aperiodic fluctuations possibly exhibit chaotic behaviour. Furthermore, the transitions of the system dynamics, from aperiodic to periodic oscillations and vice versa, can be clearly detected by the recurrence quantification measures such as $\%DET$ and L_{max} during intermittency. The characterization of type of intermittency demonstrates the presence of type-II intermittency in the dynamics of the spray combustion system.

The bifurcation study of the acoustic pressure oscillations demonstrates the presence of higher amplitude bursts during intermittency compared to that during limit cycle oscillations. The maximum amplitude of such bursts can grow as high as three times that of the sustained periodic oscillations. The presence of these high amplitude intermittent loads during intermittency may be more dangerous to the system components than the low amplitude continuous cyclic loads observed during limit cycle oscillations. A sudden jump in the pressure amplitude can cause fracture of the brittle materials or can lead to deformation of the ductile materials. Sometimes, the damage caused by a single burst cannot be recognized easily but the continuous exposure of different amplitude intermittent loads over a long-term operation can lead to fatigue failure of the system parts. As a result, the intermittent oscillations wherein the high amplitude bursts occur pose a major challenge to the engine operator to protect the system before reaching a state of sustained limit cycle oscillations. Such behaviour of intermittent oscillations might be present in the practical combustion systems and should be considered during the construction of models of the thermoacoustic systems.

Acknowledgements We gratefully acknowledge Prof. M. V. Panchagnula for the valuable guidance provided during the course of development of the experimental set-up. We are grateful to Mr. R. Vishnu and Dr. M. Vadivukkarasan for the help provided in performing the experiments and for the fruitful discussion on the obtained results. This work has been supported by Defence Research & Development Organization (DRDO), India. We would like to thank Dr. V. Ramanujachari and Mr. S. Manikandan from RIC, DRDO.

References

Abarbanel HD, Brown R, Sidorowich JJ, Tsimring LS (1993) The analysis of observed chaotic data in physical systems. Rev Mod Phys 65(4):1331

Ananthkrishnan N, Deo S, Culick FE (2005) Reduced-order modeling and dynamics of nonlinear acoustic waves in a combustion chamber. Combust Sci Technol 177(2):221–248

Anderson W, Miller K, Ryan H, Pal S, Santoro R, Dressler J (1998) Effects of periodic atomization on combustion instability in liquid-fueled propulsion systems. J Propul Power 14(5)

Candel S (2002) Combustion dynamics and control: progress and challenges. Proc Combust Inst 29(1):1–28

Cao L (1997) Practical method for determining the minimum embedding dimension of a scalar time series. Phys D Nonlin Phenomena 110(1–2):43–50

Carvalho J, Ferreira M, Bressan C, Ferreira J (1989) Definition of heater location to drive maximum amplitude acoustic oscillations in a rijke tube. Combust Flame 76(1):17–27

Chatterjee S, Mallik A (1996) Three kinds of intermittency in a nonlinear mechanical system. Phys Rev E 53(5):4362

Chishty WA (2005) Effects of thermoacoustic oscillations on spray combustion dynamics with implications for lean direct injection systems. Ph.D. Thesis, Virginia Tech

Culick F (1988) Combustion instabilities in liquid-fuelled propulsion systems

Culick F, Kuentzmann P (2006) Unsteady motions in combustion chambers for propulsion systems. Technical Report, Nato Research and Technology Organization Neuilly-SUR-SEINE (France)

Dattarajan S, Lutomirski A, Lobbia R, Smith O, Karagozian A (2006) Acoustic excitation of droplet combustion in microgravity and normal gravity. Combust Flame 144(1):299–317

Domen S, Gotoda H, Kuriyama T, Okuno Y, Tachibana S (2015) Detection and prevention of blowout in a lean premixed gas-turbine model combustor using the concept of dynamical system theory. Proc Combust Inst 35(3):3245–3253

Dubey R, McQuay M, Carvalho J (1998) An experimental and theoretical investigation on the effects of acoustics on spray combustion. In: Symposium (International) on Combustion, vol. 27, pp 2017–2023. Elsevier

Ducruix S, Schuller T, Durox D, Candel S (2003) Combustion dynamics and instabilities: elementary coupling and driving mechanisms. J Prop Power 19(5):722–734

Duvvur A, Chiang C, Sirignano W (1996) Oscillatory fuel droplet vaporization-driving mechanism for combustion instability. J Prop Power 12(2):358–365

Eckmann JP, Kamphorst SO, Ruelle D (1987) Recurrence plots of dynamical systems. EPL (Europhysics Letters) 4(9):973

Elaskar S, Del Río E (2017) New advances on chaotic intermittency and its applications. Springer

Feng D, Zheng J, Huang W, Yu C, Ding W (1996) Type-i-like intermittent chaos in multicomponent plasmas with negative ions. Phys Rev E 54(3):2839

Frank M, Schmidt M (1997) Time series investigations on an experimental system driven by phase transitions. Phys Rev E 56(3):2423

Fraser AM, Swinney HL (1986) Independent coordinates for strange attractors from mutual information. Phys Rev A 33(2):1134

Gotoda H, Shinoda Y, Kobayashi M, Okuno Y, Tachibana S (2014) Detection and control of combustion instability based on the concept of dynamical system theory. Phys Rev E 89(2), 022,910

Griffith T, Parthimos D, Crombie J, Edwards DH (1997) Critical scaling and type-iii intermittent chaos in isolated rabbit resistance arteries. Phys Rev E 56(6):R6287

Hammer PW, Platt N, Hammel SM, Heagy JF, Lee BD (1994) Experimental observation of on-off intermittency. Phys Rev Lett 73(8):1095

Hasson CJ, Van Emmerik RE, Caldwell GE, Haddad JM, Gagnon JL, Hamill J (2008) Influence of embedding parameters and noise in center of pressure recurrence quantification analysis. Gait Post 27(3):416–422

Hilborn RC (2000) Chaos and nonlinear dynamics: an introduction for scientists and engineers. Oxford University Press on Demand

Kabiraj L, Paschereit CO, Gutmark E (2016) Analysis of combustion oscillations in a staged mldi burner using decomposition methods and recurrence analysis
Kabiraj L, Saurabh A, Wahi P, Sujith R (2012) Route to chaos for combustion instability in ducted laminar premixed flames. Chaos Interdisc J Nonlin Sci 22(2), 023,129
Kabiraj L, Sujith R (2012) Nonlinear self-excited thermoacoustic oscillations: intermittency and flame blowout. J Fluid Mech 713:376–397
Kantz H, Schreiber T (2004)Nonlinear time series analysis, vol. 7. Cambridge University Press
Kashinath K, Waugh IC, Juniper MP (2014) Nonlinear self-excited thermoacoustic oscillations of a ducted premixed flame: bifurcations and routes to chaos. J Fluid Mech 761:399–430
Kennel MB, Brown R, Abarbanel HD (1992) Determining embedding dimension for phase-space reconstruction using a geometrical construction. Phys Rev A 45(6):3403
Klimaszewska K, Żebrowski JJ (2009) Detection of the type of intermittency using characteristic patterns in recurrence plots. Phys Rev E 80(2), 026,214
Kumagai S, Isoda H (1955) Combustion of fuel droplets in a vibrating air field. In: Symposium (International) on Combustion, vol. 5, pp 129–132. Elsevier
Lei S, Turan A (2009) Nonlinear/chaotic analysis, modelling and control of combustion instabilities due to vaporizing sprays. Chaos, Solitons & Fract 42(3):1766–1779
Lieuwen T (2005) Online combustor stability margin assessment using dynamic pressure data. Trans ASME-A-Eng Gas Turbines Power 127(3):478–482
Lieuwen TC (2002) Experimental investigation of limit-cycle oscillations in an unstable gas turbine combustor. J Prop Power 18(1):61–67
Lieuwen TC (2012) Unsteady combustor physics. Cambridge University Press
Lieuwen TC, Yang V (2005) Combustion instabilities in gas turbine engines (operational experience, fundamental mechanisms and modeling). Progress in astronautics and aeronautics
Marwan N, Romano MC, Thiel M, Kurths J (2007) Recurrence plots for the analysis of complex systems. Phys Rep 438(5):237–329
McManus K, Poinsot T, Candel S (1993) A review of active control of combustion instabilities. Prog Energy Combust Sci 19(1):1–29
Muugesan M, Sujith R (2015) Intermittency in combustion dynamics. In: 51st AIAA/SAE/ASEE Joint Propulsion Conference, p. 3967
Nair V, Sujith R (2013) Identifying homoclinic orbits in the dynamics of intermittent signals through recurrence quantification. Chaos Interdisc J Nonlin Sci 23(3), 033–136
Nair V, Sujith R (2014) Multifractality in combustion noise: predicting an impending combustion instability. J Fluid Mech 747:635–655
Nair V, Thampi G, Karuppusamy S, Gopalan S, Sujith R (2013) Loss of chaos in combustion noise as a precursor of impending combustion instability. Int J Spray Combust Dynam 5(4):273–290
Nair V, Thampi G, Sujith R (2014) Intermittency route to thermoacoustic instability in turbulent combustors. J Fluid Mech 756:470–487
Okai K, Moriue O, Araki M, Tsue M, Kono M, Sato J, Dietrich D, Williams F (2000) Combustion of single droplets and droplet pairs in a vibrating field under microgravity. Proc Combust Inst 28(1):977–983
Pawar SA, Vishnu R, Vadivukkarasan M, Panchagnula MV, Sujith R (2015) Intermittency route to combustion instability in a laboratory spray combustor. ASME Turbo Expo Power for Land, Sea, and Air (GT2015-42919)
Pawar SA, Vishnu R, Vadivukkarasan M, Panchagnula MV, Sujith RI (2016) Intermittency route to combustion instability in a laboratory spray combustor. J Eng Gas Turbines Power 138(4), 041,505
Pomeau Y, Manneville P (1980) Intermittent transition to turbulence in dissipative dynamical systems. Commun Math Phys 74(2):189–197
Rayleigh JWS (1878) The explanation of certain acoustical phenomena. Nature 18(455):319–321
Ringuet E, Rozé C, Gouesbet G (1993) Experimental observation of type-ii intermittency in a hydrodynamic system. Phys Rev E 47(2):1405

Sacher J, Elsässer W, Göbel EO (1989) Intermittency in the coherence collapse of a semiconductor laser with external feedback. Phys Rev Lett 63(20):2224
Saito M, Hoshikawa M, Sato M (1996) Enhancement of evaporation/combustion rate coefficient of a single fuel droplet by acoustic oscillation. Fuel 75(6):669–674
Schuster HG, Just W (2006) Deterministic chaos: an introduction. Wiley
Smith DA, Zukoski EE (1985) Combustion instability sustained by unsteady vortex combustion
Sterling J, Zukoski E (1987) Longitudinal mode combustion instabilities in a dump combustor
Subramanian P (2011) Dynamical systems approach to the investigation of thermoacoustic instabilities
Sujith R (2005) An experimental investigation of interaction of sprays with acoustic fields. Exp Fluids 38(5):576–587
Sujith R, Juniper M, Schmid P (2016) Non-normality and nonlinearity in thermoacoustic instabilities. Int J Spray Combust Dynamics 8(2):119–146
Sujith R, Waldherr G, Jagoda J, Zinn B (1997) An experimental investigation of the behavior of droplets in axial acoustic fields. J Vib Acoust 119:285–292
Takens F et al (1981) Detecting strange attractors in turbulence. Lecture Notes Math 898(1):366–381
Tanabe M, Morita T, Aoki K, Satoh K, Fujimori T, Sato J (2000) Influence of standing sound waves on droplet combustion. Proc Combust Inst 28(1):1007–1013
Theiler J, Eubank S, Longtin A, Galdrikian B, Farmer JD (1992) Testing for nonlinearity in time series: the method of surrogate data. Phys D Nonlin Phenom 58(1–4):77–94
Unni VR, Sujith R (2015) Multifractal characteristics of combustor dynamics close to lean blowout. J Fluid Mech 784:30–50
Unni VR, Sujith R (2017) Flame dynamics during intermittency in a turbulent combustor. Proc Combust Inst 36(3):3791–3798
Webber CL, Zbilut JP (1994) Dynamical assessment of physiological systems and states using recurrence plot strategies. J Appl Physiol 76(2):965–973
Xiao Y, Wang Y, Lai YC (2009) Dependence of intermittency scaling on threshold in chaotic systems. Phys Rev E 80(5), 057,202
Young V (1995) Liquid rocket engine combustion instability, vol. 169. Aiaa
Zbilut JP, Webber CL (1992) Embeddings and delays as derived from quantification of recurrence plots. Phys Lett A 171(3–4):199–203